

## Shape-controlled Synthesis of Octahedral Gold Nanocrystals in the Poly(*N*-vinyl-2-pyrrolidone) Matrix via Reduction of HAuCl<sub>4</sub>

Mari Yamamoto,<sup>1</sup> Yukiyasu Kashiwagi,<sup>1</sup> Takao Sakata,<sup>2</sup> Hirotarō Mori,<sup>2</sup> and Masami Nakamoto<sup>\*1</sup>

<sup>1</sup>Osaka Municipal Technical Research Institute, 6-50, 1-Chome, Morinomiya, Joto-ku, Osaka 536-8553

<sup>2</sup>Research Center for Ultra-High Voltage Electron Microscopy, Osaka University, Yamada-oka, Suita, Osaka 565-087

(Received August 1, 2007; CL-070817; E-mail: nakamoto@omtri.city.osaka.jp)

Single-crystalline octahedral gold nanocrystals bounded by {111} facets were obtained as a major product via the reduction of HAuCl<sub>4</sub> in poly(*N*-vinyl-2-pyrrolidone) matrix by the control of the heating temperatures and PVP/Au ratios.

Control of the morphology of metal nanocrystals with well-defined shapes has received intense attention due to the interest of electronic, optical, magnetic, and catalytic properties.<sup>1</sup> Concerning with the methods of shape-controlled synthesis, two approaches have been mainly used. One is the template-directed method. The reduction of metal ions in solutions is carried out in the presence of solid templates, such as mesoporous inorganic materials,<sup>2</sup> polymers,<sup>3</sup> and carbon nanotubes.<sup>4</sup> The other is the crystal growth method. The key point of this method is selective interaction between the capping ligands, such as surfactants, polymers, and small molecules, and the specific face of nanocrystals to avoid the growth of their facets. Using this method, various shapes of gold and silver nanocrystals including plates,<sup>5</sup> rods,<sup>6</sup> blanchard nanocrystals,<sup>7,8</sup> and cubes<sup>9</sup> have been prepared in solutions. However, reports concerning octahedral gold nanocrystals have been very limited<sup>10,11</sup> and the preparative condition requires higher heating temperature of 250 °C.<sup>11</sup>

Here, we report shape-controlled synthesis of gold nanocrystals in the poly(*N*-vinyl-2-pyrrolidone) (PVP) matrix via the reduction of HAuCl<sub>4</sub>. The anisotropic growth of gold nanocrystals was promoted in the polymer matrix rather than in solution.<sup>12</sup> Because the slow diffusion<sup>13</sup> of gold atoms and the protection of gold atoms by PVP have been achieved in the polymer matrix to avoid rapid aggregation, resulting the single-crystalline octahedral nanocrystals bounded by {111} facets as a major product by controlling the reaction conditions of heating temperature and PVP/Au ratio.

A series of PVP matrix including gold ions was prepared by drying the mixture of aqueous solutions of HAuCl<sub>4</sub> and PVP ( $M_w = 40,000$ ) at 50 °C for 30 min on a glass substrate (molar ratio of repeating unit of PVP/Au = 5, 10, 25). The reduction of gold ions in the PVP matrix was conducted by heating from 50 °C under the condition of 2 °C/min and held at 125 °C for 24 h, 150 °C for 2 h, and 170 °C for 1 and 24 h, respectively. The color of the matrix changed from pale yellow to reddish violet. The completion of the reduction of gold ions was confirmed by the disappearance of their absorption at 320 nm. The reduction of gold ions may proceed by the reducing action of macroradicals formed during degradation of PVP by radicals derived from hydroxyl peroxide, which remained in commercially available PVP.<sup>14a</sup>

The XRD pattern of the obtained PVP matrix shows sharp peaks corresponding to the {111}, {200}, and {220} diffraction peaks of Au<sup>0</sup>, which demonstrates the formation of crystalline

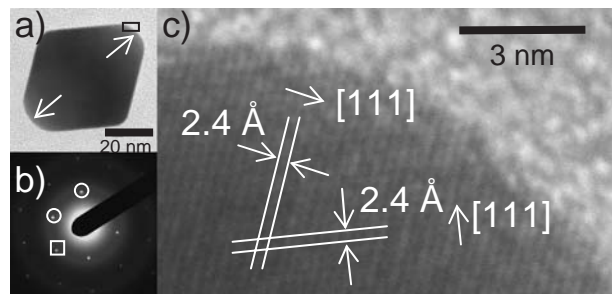


**Figure 1.** a) TEM image of an octahedral gold nanocrystal. The arrows show [100] directions. b) Corresponding electron diffraction pattern taken with the incident beam perpendicular to the panel (a). The spots (boxed and circled) could be indexed as the {200} and {111} diffractions, respectively. c) HRTEM image of the edge of the octahedral gold nanocrystal as marked by a black frame shown in panel (a).

Au<sup>0</sup> with face-centered cubic (fcc) structure. In addition, the UV–vis absorption spectrum of PVP matrix obtained under the condition of PVP/Au = 10 at 125 °C shows a relatively sharp plasmon absorption at 547 nm, similar to that of PVP-capped gold nanoparticles with similar size. This indicates that the gold nanocrystals are well dispersed in the PVP matrix. The morphologies of the gold nanocrystals were characterized by transmission electron microscopy (TEM), selected-area electron diffraction (SAED), and high-resolution TEM (HRTEM). Comparing with the present polymer matrix method, the reduction of gold ions in the presence of PVP in aqueous solution afforded mixture of spherical nanoparticles, plates, and multiple-twinned particles.<sup>14</sup>

To clarify the 3D shape of gold nanocrystals by TEM (Figure S1a, see Supporting Information),<sup>16</sup> the observations at five different angles, 45, 20, 0, –20, and –45°, were performed by tilting the sample holder (Figure S1b–S1d), respectively.<sup>16</sup> As a result, the ratios of nanocrystals obtained under the condition of PVP/Au = 10 at 125 °C are octahedron (77%), disordered multiple twin (DMT) (vide infra) (15%), triangular plate (4%), decahedron (2%), and irregular shapes (2%), respectively.

SAED and HRTEM were performed to investigate the morphologies of the nanocrystals precisely. The octahedral nanocrystal (Figure 1a) was perpendicularly incident by electron beam for taking the SAED pattern (Figure 1b). Taking account of the spots indicated by a box and circles corresponding to the {200} and {111} lattice planes of fcc gold, respectively, it is estimated the zone axis is [110]. Compared with the TEM image (Figure 1a), it is revealed that the octahedral nanocrystal is a single crystal bounded by {111} facets and its two corners point toward the [100] directions. HRTEM image (Figure 1c) also supports the results of the SAED pattern. The HRTEM image taken

**Table 1.** Ratios of shape under the different conditions of temperatures, PVP/Au, and times

Entry	Temperature/°C	PVP/Au	Time/h	Ratio/%		
				Octahedron	DMT	Others <sup>a</sup>
1	125	10	24	77	15	8
2	150	10	2	65	25	10
3	170	10	1	40	54	6
4	170	10	24	39	61	0
5	170	25	24	21	79	0
6	170	5	1	75	13	12

<sup>a</sup>Others contain triangular plate, decahedron, and irregular shapes.

from the [110] direction shows the lattice planes continuously extend to the whole nanocrystal without stacking faults or twins, indicating a single crystal. The lattice fringes are separated by 2.4 Å corresponding (111) planes of fcc gold. In addition, the fringes face parallel to the four sides of the octahedral nanocrystal (Figure 1a). These results also suggest that the octahedral nanocrystal is bounded by {111} facets.

HRTEM and SAED pattern of DMT indicate that DMT is composed of thin and fine crystals and disordered twins with six boundaries between six triangular crystals (Figure S2).<sup>16</sup> On the other hand, the triangular nanoplate and the decahedron are twin with boundary parallel to the (111) planes between the top and bottom (Figure S3)<sup>16</sup> and multiple twin composed of five tetrahedral crystals bounded by {111} facets (Figure S4),<sup>16</sup> respectively. Most of the obtained polyhedral gold nanocrystals were bounded by the {111} facets, because of the lowest surface energy ( $\gamma_{(111)} < \gamma_{(100)} < \gamma_{(110)}$ )<sup>15</sup> and selective adsorption of PVP to {111} facets of gold nanocrystals.<sup>10a,14</sup>

The reaction conditions were investigated to clarify the effect of temperatures and PVP/Au ratios for the ratio of octahedron (Table 1). When the temperatures of heating treatment became higher under the condition of PVP/Au = 10, the shorter heating time was enough to complete the reaction (Table 1, Entries 1–3). Furthermore, the heating time did not affect the ratio of shape, based on the results under the condition of 170 °C for 1 h and for 24 h (Table 1, Entries 3 and 4). As the temperature increased from 125 to 150 and 170 °C, the ratio of octahedron decreased from 77% to 65% and 40%, respectively (Table 1, Entries 1–3). While the average size of octahedron defined as opposite side distance became larger from  $12 \pm 2$  to  $13 \pm 2$  and  $33 \pm 5$  nm, respectively, because of faster nucleation and faster growth at higher temperature.

As the PVP/Au ratios decreased from 25 to 5 under the condition at 170 °C (Table 1, Entries 3–6), the ratio of octahedron increased up to 75% for PVP/Au = 5 (Figure S5).<sup>16</sup> While the average size of octahedron became larger from  $27 \pm 6$  to  $66 \pm 10$  nm. In the case of PVP/Au = 2, the aggregated bulk gold was produced because the amount of PVP was not enough to avoid the rapid aggregation of gold nanoparticles. Therefore, the ratio of the octahedron increase under the conditions at lower temperatures or of lower PVP/Au ratios.

As described above, PVP acts as mild reducing agent. Thus, the higher PVP/Au ratio causes rapid nucleation to produce the crystals with stacking faults, inducing twinned structure, DMT. On the other hand, the lower PVP/Au ratio causes slower nucleation to form the single-crystalline seeds and rapid growth to afford the octahedral nanocrystals.

Thus, single-crystalline seeds were formed through the slow

nucleation under the condition of lower temperature and lower PVP/Au ratio and grew to become single-crystalline octahedral nanocrystals in the present work. These correspond to the well-known results that the final structure of nanocrystals strongly depends on the initial structure of seeds.<sup>15</sup>

In summary, the anisotropic growth of gold nanocrystals was promoted in the PVP matrix via the reduction of HAuCl<sub>4</sub>. This synthetic procedure is very simple and easily produces single-crystalline octahedral gold nanocrystals bounded by {111} facets as a major product by controlling the conditions of heating temperatures and PVP/Au ratios.

This work was supported by KAKENHI (No. 18710080).

## References and Notes

- a) Y. Xia, N. J. Halas, *Mater. Res. Soc. Bull.* **2005**, *30*, 338. b) C. J. Murphy, *Science* **2002**, *298*, 2139. c) P. V. Kamat, *J. Phys. Chem. B* **2002**, *106*, 7729. d) M. A. El-Sayed, *Acc. Chem. Res.* **2001**, *34*, 257.
- Y. J. Han, J. M. Kim, G. D. Stucky, *Chem. Mater.* **2000**, *12*, 2068.
- S. T. Selvan, T. Hayakawa, M. Nogami, M. Möller, *J. Phys. Chem. B* **1999**, *103*, 7441.
- J. Sloan, D. M. Wright, S. Bailey, G. Brown, A. P. E. York, K. S. Coleman, M. L. H. Green, D. M. Wright, J. L. Hutchison, H.-G. Woo, *Chem. Commun.* **1999**, 699.
- N. Malikova, I. Pastoriza-Santos, M. Schierhorn, N. A. Kotov, L. M. Liz-Marzán, *Langmuir* **2002**, *18*, 3694.
- K. Esumi, K. Matsuhisa, K. Torigoe, *Langmuir* **1995**, *11*, 3285.
- S. Chen, Z. L. Wang, J. Ballato, S. H. Foulger, D. L. Carroll, *J. Am. Chem. Soc.* **2003**, *125*, 16186.
- M. Yamamoto, Y. Kashiwagi, T. Sakata, H. Mori, M. Nakamoto, *Chem. Mater.* **2005**, *17*, 5391.
- a) Y. Sun, Y. Xia, *Science* **2002**, *298*, 2176. b) T. S. Ahmadi, Z. L. Wang, T. C. Green, A. Henglein, M. A. El-Sayed, *Science* **1996**, *272*, 1924.
- a) M. Tsuji, N. Miyamae, S. Lim, K. Kimura, X. Zhang, S. Hikino, M. Nishio, *Cryst. Growth Des.* **2006**, *6*, 1801. b) D. Seo, J. C. Park, H. Song, *J. Am. Chem. Soc.* **2006**, *128*, 14863.
- J. Zhang, Y. Gao, R. A. Alvarez-Puebla, J. M. Buriak, H. Fenniri, *Adv. Mater.* **2006**, *18*, 3233.
- a) J.-U. Kim, S.-H. Cha, K. Shin, J. Y. Jho, J.-C. Lee, *Adv. Mater.* **2004**, *16*, 459. b) S. Porel, S. Singh, T. P. Radhakrishnan, *Chem. Commun.* **2005**, 2387.
- a) T. Herricks, J. Chen, Y. Xia, *Nano Lett.* **2004**, *4*, 2367. b) A. Chernov, *Sov. Phys.-Crystallogr.* **1972**, *16*, 734.
- a) C. E. Hoppe, M. Lazzari, I. Pardiñas-Blanco, M. A. López-Quintela, *Langmuir* **2006**, *22*, 7027. b) M. Zhou, S. Chen, H. Sun, X. Liu, *Chem. Lett.* **2007**, *36*, 652. c) M. Zhou, S. Chen, S. Zhao, *J. Phys. Chem. B* **2006**, *110*, 4510.
- B. Wiley, Y. Sun, J. Chen, H. Cang, Z. Li, X. L. Y. Xia, *Mater. Res. Soc. Bull.* **2005**, *30*, 356.
- Supporting Information is available electronically on the CSJ-Journal Web site. <http://www.csj.jp/journals/chem-lett/>.